Accepted Manuscript

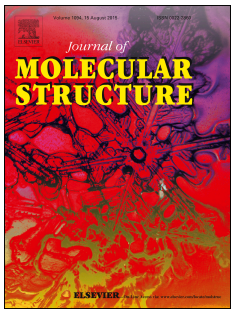

Triphenylamine-based fluorescent NLO phores with ICT characteristics: Solvatochromic and theoretical study

Santosh B. Katariya, Dinesh Patil, Lydia Rhyman, Ibrahim A. Alswaidan, Ponnadurai Ramasami, Nagaiyan Sekar

PII: S0022-2860(17)31151-1

DOI: 10.1016/j.molstruc.2017.08.084

Reference: MOLSTR 24222

To appear in: *Journal of Molecular Structure*

Received Date: 7 January 2017

Revised Date: 1 August 2017

Accepted Date: 23 August 2017

Please cite this article as: S.B. Katariya, D. Patil, L. Rhyman, I.A. Alswaidan, P. Ramasami, N. Sekar, Triphenylamine-based fluorescent NLO phores with ICT characteristics: Solvatochromic and theoretical study, *Journal of Molecular Structure* (2017), doi: 10.1016/j.molstruc.2017.08.084.

Triphenylamine-based fluorescent NLO phores with ICT characteristics: Solvatochromic and Theoretical study

Santosh B Katariya[1], Dinesh Patil[1], Lydia Rhyman[2], Ibrahim A. Alswaidan, Ponnadurai Ramasami[2], Nagaiyan Sekar[1]

Graphical Abstract:

Triphenylamine-based fluorescent NLO phores with ICT characteristics: Solvatochromic and Theoretical study

Santosh B Katariya[a], Dinesh Patil[a], Lydia Rhyman[b,c,d], Ibrahim A. Alswaidan[e], Ponnadurai Ramasami[b,c], Nagaiyan Sekar[a]

[a]Department of Dyestuff Technology, Institute of Chemical Technology, N. P. Marg, Matunga, Mumbai (MH) India-400019

[b]Computational Chemistry Group, Department of Chemistry, Faculty of Science University of Mauritius, Réduit 80837, Mauritius.

[c]Department of Applied Chemistry, University of Johannesburg, Doornfontein Campus, Johannesburg 2028, South Africa

[d]Department of Chemistry, University of Johannesburg, PO Box 524, Auckland Park, Johannesburg, 2006, South Africa

[e]Department of Pharmaceutical Chemistry, College of Pharmacy, King Saud University, Riyadh 11451, Saudi Arabia

Email: n.sekar@ictmumbai.edu.in, nethi.sekar@gmail.com, ramchemi@intnet.mu

[a]Tel.: +91 22 3361 1111/ 2707; Fax.: +91 22 3361 1020

[b]Tel.: +230 403 7507; Fax.: +230 465 6928

Abstract:

The static first and second hyperpolarizability and their related properties were calculated for triphenylamine-based "push-pull" dyes using the B3LYP, CAM-B3LYP and BHHLYP functionals in conjunction with the 6-311+G(d,p) basis set. The electronic coupling for the electron transfer reaction of the dyes were calculated with the generalized Mulliken-Hush method. The results obtained were correlated with the polarizability parameter α_{CT}, first hyperpolarizability parameter β_{CT}, and the solvatochromic descriptor of $\langle\gamma\rangle_{SD}$ obtained by the solvatochromic method. The dyes studied show a high total first order hyperpolarizability (70 to 238 times) and second order hyperpolarizability (412 to 778 times) compared to urea. Among the three functionals, the CAM-B3LYP and BHHLYP functionals show hyperpolarizability values closer to experimental values. Experimental absorption and emission wavelengths measured for all the synthesized dyes are in good agreement with those predicted using the time-dependent density functional theory. The theoretical examination on non-linear optical properties was

performed on the key parameters of polarizability and hyperpolarizability. A remarkable increase in non-linear optical response is observed on insertion of benzothiazole unit compared to benzimidazole unit.

Introduction

Non-linear optic (NLO) deals with the interactions of applied electromagnetic fields with materials to yield new optical properties such as electromagnetic fields, altered frequency, phase, and amplitude [1,2]. The search for efficient organic non-linear optical (NLO) materials has been of interest in both academia and industry because of their potential applications in the design of photon-based materials for optical switching, information processing, and data manipulation [3,4]. The molecular structure of organic NLO materials is based on the π bond system. The overlap of π orbital and delocalization of electronic charge distribution lead to a high mobility of the electron density. Functionalization of both ends of the π system with appropriate electron donor and acceptor groups can enhance the asymmetric electronic distribution in either or both ground and excited states leading to an increased optical non-linearity [5,6]. NLO materials have good non-linear susceptibilities but low laser damage threshold than inorganic counter parts [7]. Conjugated organic molecules have some advantages over inorganic molecules as they possess low dielectric constant, small refractive indices, faster response time and they crystalize in non–centrosymmetric system [8]. Large second-order non-linearities can be obtained from the NLO materials containing a push-pull type chromophore which possesses large dipole moments and polarizabilities and consisting of strong electron-donating and-withdrawing groups linked by a π-delocalized moiety [9]. Such types of molecules have a distinctive figure of merit given as $\frac{\mu\times\beta}{MW}$ where μ is the dipole moment, β is the first hyperpolarizability and MW the molecular weight of the chromophore [10]. On the basis of experimental and theoretical studies, the design of second-order NLO materials to create large hyperpolarizability has primarily focused on the following: (a) the planar D–π–A model [11], (b) auxiliary donors and acceptors model of heterocycle [12,13] and (c) twisted π-electron systems [14–16].

There are experimental and theoretical methods reported to evaluate β. A common experimental method used to obtain β is to polarize the sample dissolved in a non-polar solvent with a strong electric field in order to induce molecular alignment. A laser beam is sent through the solution and the intensity of second harmonic generation (SHG) is measured. This method for evaluating the second-order molecular polarizability is the electric field induced second harmonic

generation (EFISH) [17]. Another technique is the hyper-Rayleigh scattering (HRS) [18]. These two methods are expensive and they require sophisticated experimental set up and trained manpower to handle the instruments. The solvatochromic method is not only a simple practice but it is also cost-effective. This method used for the determination of the first order hyperpolarizability (β_{ijk} or β_{xxx} or β_{CT}) was successfully applied first by Paley *et al*. [19]. The solvent dependent absorption and emission properties throw light on the nature of the excited state and hence the solvatochromic method is used to understand the NLO properties which mainly are the manifestations of the excited state nature of an organic molecule [20,21]. In this work, we have used the solvatochromic method in which only the absorption/emission data is required for the two level microscopic model of β based on the Oudar formulae [22]. The solvatochromic method gives only the dominant tensor component of hyperpolarizability, i.e. β_{ijk} assuming that the charge-transfer in a donor-acceptor molecule takes place along the axis of the permanent ground state dipole moment [19] and thus the two level microscopic model of β will give the β_{xxx} or β_{CT}. Besides the solvatochromic method, in the past few decades theoretical computations have become a priori tool to compute the NLO properties of organic materials [23,24]. Computational methods are useful in having prior understanding of the structure in relation to the properties and the factors governing the efficiency of NLO properties, such as the contribution of the donor-acceptor and solvent effects. The hyperpolarizability of the molecule is largely influenced by the contribution from the higher excited states particularly the first excited state in addition to the ground state [25,26].

In an attempt to understand the organic NLO materials, we were interested in triphenylamine derivatives since triphenylamine is unique and widely accepted donating group due to its very good electron donating ability and its charge-transfer characteristic has been known to exhibit rigid plane, long conjugation length and good hole transporting properties [27]. Thus triphenylamine and its derivatives display promising properties in the development of light emitting [28], organic field-effect transistors (OFET) [29], photovoltaic devices [30] and dye-sensitized solar cells [27]. In addition, electron transfer or electron separation between the triphenylamine and the accepting group provides this class of compounds highly anisotropic structures and interesting photo physical properties [31]. Gao *et al*. reported a range of triphenylamine-based derivatives with various substituent groups [32]. It was reported that the introduction of heteroatom to the benzene ring of the triarylamine donor can efficiently improve

the electron-donating ability, which improves the hyperpolarizability [33,34]. In the current decade several research groups have achieved the large second-order NLO response by extending the conjugated bridge through π-spacer [9,35–37]. The modulation of non-linear optical properties by attaching various strong electron-withdrawing groups to a triphenylamine backbone are reported in literature [38,39]. Recently, Zhou *et al.* showed that the introduction of benzimidazole derivatives in the phenyl ring of the triphenylamine core increases the molar extinction coefficients together with absorption maxima (due to the increased π-conjugation) when compared to the un-substituted counterpart [40].

In view of the above, in this work, we synthesized two triphenylamine-based dyes namely, TPA BIZ and TPA BTZ [41] as they have intramolecular charge transfer (ICT) characteristics. We also shed light into the effect of benzothiazole and benzimidazole group of the π-conjugated system in terms of the photo-physical characterization and non-linear optical (NLO) properties of triphenylamine-based dyes. We used the solvatochromic two level microscopic model to obtain the polarizability parameter α_{CT}, first hyperpolarizability parameter (β_{CT}), and solvatochromic descriptor of $\langle \gamma \rangle_{SD}$. The static first hyperpolarizability (β_0) and its related properties (μ, α_0, $\Delta\alpha$, β, $\bar{\gamma}$) (μ measured in Debye and other quantities in *esu*) were determined using density functional theory (DFT) and time-dependent DFT (TD-DFT) methods .

< **Please insert Fig.1** Synthesis of TPA BIZ and TPA BTZ >

Methodology

All the chemicals were purchased from Sigma Aldrich and S. D. Fine Chemicals Ltd, Mumbai, India. The solid reagents were characterized by melting points and used without further purification. The liquid reagents were distilled at their boiling points and used without any further purification. Solvents were used after distillation at their boiling point and drying according to standard processes. All the reactions were monitored on pre-coated silica gel aluminium based plates kisel gel 60 F254 Merck, India. Purification of all the dyes was achieved by recrystallization. Melting points were recorded on instrument from Sunder Industrial Product Mumbai by using open capillary and are uncorrected. The absorption spectra of the dyes were recorded on a Lambda 25 UV-Visible spectrophotometer. ^{1}H NMR spectra were recorded on a Varian Cary Eclipse Australia. The chemical shift values are expressed in δ ppm using $CDCl_3$ as

a solvent and chemical shifts are reported relative to tetramethylsilane (Me_4Si) (δ=0.0) as an internal standard.

Synthesis of compound TPA BIZ

To a stirring solution of *o*-phenylenediamine (108 mg, 1.0 mmol) in 20 ml methanol, solution of 4-(diphenylamino) benzaldehyde (273 mg, 1.0 mmol) was added drop wise through a dropping funnel. After that the mixture was heated to reflux for 4 hour. On completion of the reaction the mixture was cooled and poured into water. The resulting precipitate was filtered, washed with water and dried. The residue was chromatographed on silica gel (petroleum ether: CH_2Cl_2 = 10:1 V/V) to give the compound TPA BIZ as a milk white powder in 60% yield. Melting point 279°C (lit. 280°C)

^{1}H NMR (500 MHz, DMSO) δ 8.03 (d, *J* = 7.9 Hz, 1H), 7.94 (d, *J* = 8.1 Hz, 1H), 7.90 (d, *J* = 8.7 Hz, 2H), 7.46 (t, *J* = 7.6 Hz, 1H), 7.39 – 7.31 (m, 5H), 7.11 (dd, *J* = 15.9, 7.7 Hz, 6H), 6.95 (d, *J* = 8.7 Hz, 2H).

^{13}C NMR (126 MHz, DMSO) δ 167.36, 154.16, 150.54, 146.63, 134.58, 130.28, 128.91, 126.90, 125.90, 125.83, 125.42, 124.94, 122.80, 122.57, 121.06.

HRMS (ESI): m/z calcd for $(M + H)^+$ $C_{25}H_{19}N_3$ 362.1579; found 362.1566.

Synthesis of compound TPA BTZ

To a solution of 2-aminobenzenethiol (125 mg, 1.0 mmol) in 20 mL DMSO and 4-(diphenylamino) benzaldehyde (273 mg, 1.0 mmol) was added and the mixture was heated at 120 °C for 2 h. When the reaction was complete, the reaction mixture was cooled, poured into water and extracted with CH_2Cl_2 (90 ml). The organic layer was dried with $MgSO_4$ and the solvents were evaporated under vacuum. The residue was chromatographed on silica gel (petroleum ether: CH_2Cl_2 = 5:1 V/V) to give the compound TPA BTZ as a white powder in 75% yield. Melting Point 271°C (lit. 272°C).

^{1}H NMR (500 MHz, $CDCl_3$) δ 8.03 (d, *J* = 8.1 Hz, 1H), 7.93 (dd, *J* = 8.8, 2.3 Hz, 2H), 7.87 (d, *J* = 7.9 Hz, 1H), 7.49 – 7.45 (m, 1H), 7.37 – 7.29 (m, 5H), 7.18 (d, *J* = 7.4 Hz, 4H), 7.14 – 7.09 (m, 4H).

^{13}C NMR (126 MHz, $CDCl_3$) δ 167.81, 154.30, 150.42, 146.91, 134.82, 129.50, 128.53, 126.57, 126.16, 125.40, 124.70, 124.03, 122.77, 121.73, 121.47).

HRMS (ESI): m/z calcd for $(M + H)^+$ $C_{25}H_{18}N_2S$ 379.1109; found 379.1183.

Computational method

To get further insight into the effect of molecular structure and electron distribution on the spectroscopic properties of the TPA BIZ and TPA BTZ, their geometries and energies were optimized by DFT calculations using B3LYP/6-311+G(d,p) method [42]. TD-DFT was employed for the excited state optimization. The functionals used were B3LYP [43,44], BHHLYP [45,46] and CAM-B3LYP [47]. The hybrid functionals B3LYP and BHHLYP are based on the LYP functional for the correlation part whereas they differ by the amount of HF exchange, 20% in B3LYP and 50% in BHHLYP. The CAM-B3LYP functional comprises of 0.19 Hartree–Fock (HF) plus 0.81 Becke 1988 (B88) exchange interaction at short-range and 0.65 HF plus 0.35 B88 at long-range. The basis sets used for all atoms were the popular Pople's split-valence basis sets [48,49]. The triple zeta basis set is employed for all the three functionals with both diffuse and polarization functions, 6−311+G(d,p). The choice of the functionals is based on the fact that the charge-transfer states are better modeled with increasing amount of HF in the hybrid (B3LYP and BHHLYP) as well as range separation (CAM-B3LYP) [50]

The vibrational frequencies of the optimized structures were computed using the same method to verify that the optimized structures correspond to local minima on the energy surface. All the computations in solvents of different polarities were carried out using the self-consistent reaction field incorporated in the IEFPCM model as implemented in Gaussian 09 [51,52]. The excitation energies, oscillator strengths and orbital contribution for the lowest 10 singlet-singlet transitions at the optimized geometry in the ground state were obtained by TD-DFT calculations using the same basis set as for the geometry minimization. The static second-order polarizability or first hyperpolarizability (β) and its related properties for TPA BIZ and TPA BTZ dyes were calculated on the basis of the finite-field approach [53]. The values of Onsager cavity radii were obtained using the DFT-optimized geometries in the respective solvents by performing volume computations. All computations were performed using the Gaussian 09 software [54] operating on GridChem [55–57]. The BHHLYP and the CAM-B3LYP functionals are found to yield values of hyperpolarizabilities closer to experimental values than the B3LYP functional [58].

Electronic vertical excitation spectra (TD-DFT)

For the calculation of vertical excitations, the ground state optimized geometries were subjected to TD-DFT computations for the first 10 states using the B3LYP/6-311+G(d,p) method and the results are listed in Table 1. The results from the DFT and TD-DFT calculations support the

experimental results suggesting that there was no influence of the variation in the solvent polarity on the absorption of the TPA BIZ and TPA BTZ dyes (Table 1). The absorption spectra for the TPA BIZ and TPA BTZ dyes are shown in Fig. 2. The computed absorption wavelength for the TPA BIZ dye ranges from 380 to 381 nm while the experimental values ranges from 350 to 355 nm. For TPA BTZ dye, the computed absorption wavelength ranges from 370 to 376 nm while the experimental value is 407 nm. For TPA BIZ and TPA BTZ, the observed lowest energy absorption bands are associated to the predicted S0→S1 transitions (HOMO→LUMO); with major contribution > 97% and strong oscillator strengths ranging from 0.987 to 1.048. Both the experimental absorption and the computed vertical excitation of the compounds were correlated with each other and are independent of the solvent polarity.

< **Please insert Fig 2 Absorption and Emission spectra of TPA BIZ and TPA BTZ >**

< **Please insert Table 1 Observed absorption and computed vertical excitation for TPA BIZ and TPA BTZ >**

Emission Spectra

The experimental and computed emission spectra for the TPA BIZ and TPA BTZ dyes are shown in Fig. 2. The minimum energy S1, B3LYP-optimized structures were used for the emission computations, and the results are listed in Table 2. From the calculated emissions, it can be observed that there is little influence of solvent polarity on the emission of the TPA BIZ and TPA BTZ dyes. In case of TPA BIZ, the emission wavelength is red shifted by 1364 cm^{-1} (20 nm) from toluene to ethanol. A similar trend is observed in TPA BTZ but it is red shifted by 2309 cm^{-1} (50 nm).

The TD-DFT emission maxima calculated for all the dyes in various solvents are associated with the LUMO→HOMO transition with major contribution (>98%). The experimental emissions values range from 412 to 484 nm and the computed emissions range from 442 to 506 nm with an oscillator strength in the order of 0.274 to 0.808 (Table 2).

For the TPA BIZ and TPA BTZ dyes, the observed large Stokes shift values are found at 3696 and 3897 cm^{-1} in toluene solution and 6006 and 5261 cm^{-1} in ethanol respectively (SI Tables 1 and 2) and these points out to the occurrence of an ICT process [59–61] between the donor (triphenylamine) unit and the electron-acceptor benzimidazole or benzothiazole moiety. The experimental values are higher in ethanol than in toluene which is the sign of solvatochromism and charge-transfer. The computational values are showing opposite trend [62] (SI tables 1and

2). This is in agreement to the reported observation for triphenylamine-substituted benzimidazole derivatives where the longer wavelength absorption band around 340 nm was attributed to the charge-transfer (CT) $\pi - \pi^*$ transition from the electron-donating triphenylamine moiety to the electron-accepting benzimidazole moiety [63,64]. These are further confirmed by experimental (solvatochromic) calculations (SI tables 1 and 2).

< **Please insert Table 2 Observed emission and computed emission for TPA BIZ and TPA BTZ .dyes in various solvents**>

HOMO–LUMO energy gap

In order to explain the process of the charge-transfer, we obtained the isodensity plots showing the distributions of electron clouds of HOMO - LUMO of TPA BIZ and TPA BTZ dyes (Fig 3). Spatial distribution of molecular orbital, especially those of highest occupied molecular orbital (HOMO) and lowest unoccupied molecular orbital (LUMO) are excellent indicators of electron transport in molecular systems. The conjugated chromophores are characterized by a small HOMO–LUMO separation, which is the result of a significant degree of ICT from the end-capping electron donor groups to the efficient electron-acceptor groups through conjugated path [65]. The charge-transfer from HOMO to LUMO is determined by electron donor and electron acceptor group, which is responsible for the second order hyperpolarizability [66]. The electron density of the HOMO orbital is mainly located on the triphenylamine moiety or spreads over the entire molecule. The electron density of the LUMO shows a decrease in the electron density on the triphenylamine moiety (donor) and an increase in the electron-acceptor benzimidazole or benzothiazole unit. This behavior is in agreement with previous theoretical studies on similar electron donor−acceptor molecules where the lowest energy absorption band is associated with a charge-transfer (CT) type, $\pi - \pi^*$ transition from the HOMO to the LUMO orbitals [40,58,62]. The absorption and emission spectra of these compounds were also obtained in the nonpolar solvent toluene (see tables 1, 2) to further investigate the CT character of the lowest energy transition. Comparison between the spectroscopic features in ethanol and toluene reveals a solvent independent absorption spectra while the fluorescence emission spectra displays a clear solvent dependence with a significant bathochromic shift in the emission wavelength maxima with increasing solvent polarity. The higher solvatochromic shifts observed in the fluorescence

emission spectra compared to those in the absorption spectra suggests an excited state with stronger CT character and thus, supporting the behavior found in the electron density distribution of the LUMO for the TPA BIZ and TPA BTZ dyes [63,64].

In general, if the energy gap between the HOMO and LUMO decreases, it is easier for the electrons of the HOMO to be excited. In TPA BIZ and TPA BTZ dyes, the HOMO–LUMO energy gaps are 3.79 eV and 3.56 eV respectively in gas phase and 3.75 eV and 3.49 eV respectively in acetone (Table 3). From these values, it is clear that TPA BTZ is chemically more reactive than TPA BIZ [70]. The lowering of the HOMO–LUMO band gap is essentially a consequence of the large stabilization of the LUMO due to the strong electron-accepting ability of the electron-acceptor group.

The chemical hardness and softness of a molecule are good indicators of the chemical stability. In order to compare the stability of conformers energy was calculated. Molecules having large energy gap are known as hard and molecules having a small energy gap are known as soft molecules. Hard molecules are considered to be more stable than soft molecules .The soft molecules are more polarizable and more reactive than those which are hard because they need small energy for excitation. The hardness value of a molecule can be calculated using the formula [71],

$$\eta = \frac{(-E_{HOMO} + E_{LUMO})}{2}$$

where E_{HOMO} and E_{LUMO} are the energies of the HOMO and LUMO orbitals obtained by DFT computations.

Frontier molecular orbitals, i.e. HOMO and LUMO significantly affect the UV-Visible spectra and reactions between molecules. Variations in the energy gap change the kinetic stability, chemical hardness–softness and chemical reactivity. Thus, the HOMO–LUMO energy gap can be used for qualitative estimation of the NLO behavior of a molecule. A small energy gap leads to a high NLO optical response. The HOMO–LUMO energy gap (E_L-E_H) of the TPA BIZ and TPA BTZ dyes were calculated and are given in Table 3. These dyes would be outstanding for NLO properties as indicated by their small HOMO–LUMO energy gaps. The energy of the frontier molecular orbital of TPA BIZ and TPA BTZ dyes obtained using the B3LYP/6-311+G(d,p) method in various medium are presented in Fig S1 and S2 (SI).

< **Please insert Fig 3 Frontier molecular orbitals of TPA BIZ and TPA BTZ dyes in the ground state**>

< **Please insert Table 3 Energy of HOMO, LUMO and HOMO-LUMO gap of the TPA BIZ and TPA BTZ dyes in gas phase and solvents using TD-DFT [B3LYP/6-311+G(d,p)] method>**

Optimized Geometry

To understand the structures and origin of broad absorption of TPA BIZ and TPA BIZ dyes, the geometry of the dyes were optimized in the ground state in solvents of various polarities. The optimized structure of TPA BIZ and TPA BIZ dyes in the ground state and excited state are shown in Figs. 4 and 5. A major bond lengthening is observed between the bonds C_{27}–C_{31}, C_{29}–C_{31}, C_{40}–N_{45}, C_{40}–N_{46} by 0.033, 0.033, 0.022 and 0.034 Å and bond length shortened for the bonds C_3–N_{12}, N_{12}–C_{13}, C_{31}–C_{40}, N_{45}–C_{35} with -0.020, -0.021,-0.048 and-0.019 Å respectively in the case of TPA BIZ. While in the case of TPA BTZ and a major bond lengthening is observed between the bonds N_{12}–$C_{24,}C_{22}$–C_{31}, C_{29}–$C_{31,}$ C_{40}–S_{46}, C_{40}–N_{45} by 0.025, 0.028, 0.028, 0.023 and 0.039Å and bond length shortened for the bonds C_3–N_{12}, N_{12}–C_{13}, C_{31}–C_{40}, N_{45}–C_{35} with 0.025, 0.025, 0.043 and 0.023 Å respectively (Figs. 4and 5). The bond lengths alteration are due to the effect of the donor and the acceptor groups present in the TPA BIZ and TPA BIZ dyes This is due to the partial double-bond character on the bridge bond between triphenyl moiety and the acceptor unit caused by π-bonding interaction, thereby strengthening and shortening the bridge bond. This change in the bond length indicates that there is charge-transfer observed from triphenylamine core to benzimidazole and benzothiazole groups.

In agreement with previous studies [40], it is observed that the three benzene rings in the triphenylamine core are non-planar (with the phenyl rings of the triphenylamine chromophore displaying dihedral angles in the (145.9° to 146.1°), (148.7° to 149.0°) and (-33.9° to 34.0°), (-31.0° to -31.3°) range with respect to the plane formed by the phenyl ring connected to the benzimidazole moiety) and that the benzimidazole moiety presents a slightly distorted conformation with the phenyl linkage of the triphenylamine moiety displaying a dihedral angle in the (11.4° to 11.6°), (4.6° to 5.0°) range with respect to the plane formed by the phenyl group for the TPA BIZ and TPA BIZ dyes respectively.

< **Please insert Fig. 4 Optimized geometry parameters of TPA BIZ dye in acetone solvent in the ground state and excited state (bond length are in Å, dihedral angles are in degree)>**

< **Please insert Fig. 5 Optimized geometry parameters of TPA BTZ dye in acetone solvent in the ground state and excited state (bond length are in Å, dihedral angles are in degree)>**

Mulliken charge distribution The Mulliken charge distribution in the ground and the excited states (in acetone) of the compounds are summarized in Table S2. In the excited state of TPA BIZ, the net positive charge on the atom N_{12} increases and the net positive charge on the atom

C_2, C_{15}, C_{31} decreases while the net negative charge on C_{24} increases and the net negative charge on $C_{1,}$ $C_{3,}$ $C_{5,}$ C_{13} decreases.

In the excited state of TPA BTZ the net positive charge on the atom $N_{12,}$ C_{40} increases and the net positive charge on the atom C_2, C_{15}, C_{34} decreases while the net negative charge on $C_{6.}C_{24}$ increases and the net negative charge on $C_{1,}$ $C_{3,}$ $C_{5,}$ $C_{13,}$ C_{26} decreases which is suggestive of the charge delocalization in the molecule from the donor core to the acceptor core Fig. 6 and Table S3 (SI).

< **Please insert Fig 6 The ground state (GS) and excited state (ES) Mulliken charge (e) distribution of the compound TPA BIZ and TPA BTZ in acetone** >

Charge transfer Characteristics

An efficient charge-transfer (between donor and acceptor) leading to a characteristic charge-transfer excited state in a donor-π-acceptor chromophore is responsible for the manifestation of NLO properties [72]. Within a two-level approximation the strength of electronic coupling H_{DA} between the ground and charge-transfer excited states is related to the vertical excitation energy (ΔE_{eg}), the difference between the adiabatic dipole moments of the ground and excited states ($\Delta\mu_{eg}$), $\Delta\mu_{eg}^{D}$ is the difference in diabatic state dipole moments, and the transition dipole moment μ_{12} by the generalized Mulliken-Hush (GMH) equation [73–75]:

$$H_{DA} = \frac{\mu_{ge}\,\Delta E_{eg}}{\Delta\mu_{eg}^{D}} = \frac{\mu_{ge}\,\Delta E_{eg}}{\left(\Delta\mu_{eg}^{2}+4\mu_{ge}^{2}\right)^{1/2}} \qquad (1)$$

The adiabatic states are assumed to be composed of these three adiabatic states - a donor ground state (GS), a donor locally excited state (LE), and a charge-transfer state (CT) with the "transferring electron" localized on the acceptor. This approach has been carefully used in a few charge-transfer systems [76–78]. For weak donor-acceptor interactions, the adiabatic states are nearly equivalent to the adiabatic states, and thus it is possible to use the parameters like difference in dipole moments, transition dipole moments and the frequency of absorption obtained from the steady state absorption measurements.

$$H_{DA} = 2.06 \times 10^{-2} \frac{\sqrt{\nu_{max}\varepsilon_{max}\Delta\nu_{12}}}{R_{DA}} \quad (2)$$

where ε_{max} is the molar extinction coefficient at maximum absorption, in the units of M^{-1} cm^{-1}, and $\Delta\nu_{12}$ is the full width at half-maximum (FWHM) of charge-transfer band. In the above equation, H_{DA}, ν_{max}, and $\Delta\nu_{12}$ are in units of cm^{-1}. Equation (2) provides a simple method to calculate charge-transfer coupling from the characteristic values of the charge-transfer band in absorption spectra, and it is an experimental coupling value.

$$R_{DA} = 2.06 \times 10^{-2} \frac{\sqrt{\Delta E_{ge}\varepsilon_{max}\Delta\nu_{1/2}}}{H_{DA}} \quad (2a)$$

$$C_b^2 = \frac{1}{2}\left(1 - \sqrt{\frac{\Delta\mu_{ge}^2}{\Delta\mu_{ge}^2 + 4\mu_{ge}^2}}\right) \quad (2b)$$

The degree of delocalization or fractional degree of localization of the excess charge (C_b^2) and electronic coupling matrix (H_{DA}) for the diabatic states are expressed by equations (2) and (2a, 2b). The values of C_b^2, H_{DA} and R_{DA} were estimated from equations (2) and (2a, 2b) respectively, and summarized in Table 4. When C_b^2 is zero, there is total delocalization and when it is unity there is called total localization of the charge [53]. TPA BIZ possesses good values of degree of delocalization in different microenvironments and thus, the effective ICT characteristics at ground state rather than excited state. This observation is also supported by the ratio of dipole moment. Its values are less than unity. This indicates that in the ground state compounds are more polar than in the excited state. Out of two molecules TPA BTZ is more polar than TPA BIZ.

< **Please insert Table 4 Coupling strength (HDA), coupling distance (RDA), degree of delocalization C_b^2 and ratio of dipole moment for the TPA BIZ and TPA BTZ dyes in various solvents** >

Table 4 summarises the coupling strength of donor-acceptor fluorophores TPA BIZ and TPA BTZ. The large distribution of the CT coupling values ranging from 10453 to 12808 cm^{-1} for the TPA BIZ and TPA BTZ dyes only few such D−A pairs will likely have the strongest coupling values. The charge-transfer coupling is higher for the TPA BIZ dye in chloroform and EtOAc. However the lowest coupling is observed for the TPA BTZ dye. In case of TPA BIZ dye the lowest coupling distance is observed in EtOAc while the highest is in ethanol. Hence the above observation indicates that the coupling strength and coupling distance are important parameters for the donor charge-transfer molecules.

Solvatochromic method for determination of non-linear optical properties (NLO)

Calculation of α_{CT} from the solvatochromic data

Here we report the experimentally derived value of the linear polarizability α_{CT} of TPA BIZ and TPA BTZ dyes as obtained in the framework of the two-level model using UV-Visible absorption/emission spectroscopy was used to determine these values. The solvatochromic method was utilized for determination of dipole moment of the lowest lying charge-transfer excited state. Considering that in the TPA BIZ and TPA BIZ dyes charge-transfer direction is essentially coincident with the molecular long axis (here taken as X-axis), α_{CT} can be indicated as α_{xx}whose explicit expression is [79,80]:

$$\alpha_{CT} = \alpha_{xx} = 2\frac{\mu_{ge}^2}{E_{ge}} = \frac{2\mu_{eg}^2\lambda_{eg}}{hc} \quad (3)$$

x = direction of charge-transfer,

h = Planck's constant, (in erg s)

c = velocity of light in vacuum (in $cm\ s^{-1}$)

λ_{eg} = The wavelength of transition from the ground state to excited state,

μ_{ge} = The transition dipole moment which is related to the oscillator strength f by the following equation:

$$\mu_{eg}^2 = \frac{3e^2h}{8\pi^2mc} \times \frac{f}{\bar{\nu}_{eg}} \qquad (4)$$

Where,

m = mass of electron,

f = oscillator strength,

$\bar{\nu}_{eg}$ = Absorption frequency,

e = charge on electron,

The oscillator strength can be obtained by integrated absorption coefficient of the absorption band:

$$f = 4.32 \times 10^{-9} \int \varepsilon(\bar{\nu})\, d\bar{\nu} \qquad (5)$$

Where ε is the extinction coefficient (L mol^{-1} cm $^{-1}$) and $\bar{\nu}$ = absorption wave number in cm^{-1}

The transition dipole moment μ_{ge} and the oscillator strength (*f*) were calculated using equations (4) and (5). (The transition dipole moment obtained using Equation (4) is in esu, if all the constants are used in c.g.s units.). The values for α_{CT} were calculated and the results obtained were compared with theoretically obtained α_{CT} or α_{xx}. These are collected in Table 5.

The computational values of α_{CT} obtained by BHHLYP functional are closer to experimental values than B3LYP and CAM-B3LYP functionals. The computational values of α_{CT} are almost 1.5 to 2.0 times higher than the experimental values. This can be attributed to the approximations exercised in the computational model, as well the inherent simplifications associated with the solvatochromic methods in obtaining the ground and excited state dipole moments [81]. Furthermore the solvation model used here is also evolved with several assumptions [82]. Nonetheless the trends in the solvent system coincide with experimental values. The linear polarizability is sensitive to solvents and is evident in both the experimental and computational studies. Both dyes show higher α_{CT} values in polar solvents. There is substantial increase in of 15-21 × 10^{-24}esu to 16-25 × 10^{-24} esu experimentally but computationally no major change was observed from TPA BIZ to TPA BTZ.

< **Please insert Table 5 Linear polarizability α_{CT}calculated by solvatochromic and computed method for TPA BIZ and TPA BTZ>**

Calculation of β_{CT} from the solvatochromic data

The two-level microscopic model to determine solvent dependent hyperpolarizability is based on the Oudar equation [23,24] which in modified form can be presented as

$$\beta_{CT} = \beta_{xxx} = \frac{3}{2h^2c^2} \times \frac{\bar{\nu}_{eg}^2 \mu_{eg}^2 \Delta\mu_{CT}}{\left(\nu_{eg}^2 - \nu_L^2\right)\left(\nu_{eg}^2 - 4\bar{\nu}_L^2\right)} \ldots\ldots\ldots (6)$$

Where,

x = direction of charge-transfer,

$\hbar$ = Planck's constant (in erg s)

c = speed of light in vacuum (in cm s^{-1})

μ_{eg} = transition dipole moment,

ν_{eg} = transition frequency,

ν_L= frequency of the reference incident radiation to which the β value would be referred,

$\Delta\mu_{CT}$ = difference between the charge-transfer excited state and ground state dipole moment

The hyperpolarizability calculated by this equation is the dominant component of the hyperpolarizability tensor i.e. β_{xxx} and as the formula refers to charge-transfer transition [19], the hyperpolarizability obtained is often indicated as β_{CT} (charge-transfer). When there is no laser excitation (ν_L = 0), we get the static hyperpolarizability and Equation (6) reduces to the following equation:

$$\beta_{CT} = \beta_{xxx} = \frac{3}{2} \times \frac{\mu_{eg}^2 \Delta\mu_{CT}}{E_{ge}^2} \ldots\ldots\ldots (6a)$$

The $\Delta\mu_{CT}$ is obtained by using Equation (2) derived on the basis of McRae's theory [83,84]

$$\nu_{abs} - \nu_{em} = (\delta_{abs} - \delta_{em}) + \frac{2\Delta\mu_{CT}^2}{hca^3}\left(\frac{\varepsilon - 1}{\varepsilon + 2} - \frac{n^2 - 1}{n^2 + 2}\right) \ldots\ldots\ldots (7)$$

Where,

$\nu_{abs} - \nu_{em}$= Stokes shift in cm^{-1},

δ_{abs} - δ_{em} = differences in the vibrational energy (in cm^{-1}) of the molecule in the excited and ground state for absorption and emission,

a = cavity radius within Onsager's model (in cm),

ε = dielectric constant (L mol^{-1} cm^{-1})

n = refractive index of the solvent

a was calculated by integration of the solvent accessible surface using density functional theory optimized geometry.

Treating Equation (7) as

$$y = mx + c \qquad (8)$$

Where

$$y = \nu_{abs} - \nu_{em}$$

$$\boldsymbol{m} = \frac{2\Delta\mu_{CT}^2}{hca^3} \qquad x = \left(\frac{\varepsilon - 1}{\varepsilon + 2} - \frac{n^2 - 1}{n^2 + 2}\right)$$

$$and\ c = (\delta_{abs} - \delta_{em})$$

Using the value of slope *m*, $\Delta\mu_{CT}$ was then derived**,** finally substituting the values of $\Delta\mu_{CT}$ and μ_{ge} in Equation (7), β_{CT} or β_{xxx} is obtained. The values for first hyperpolarizability obtained using the solvatochromic method (Table 6) are based on several assumptions and thus allow only approximate estimate of dominant tensor of total hyperpolarizability along the direction of charge-transfer which is the major contributor to the total hyperpolarizability. Although the values are approximate, it has advantages over the other well-known expensive methods to understand the facts. The calculated β_{CT} values are given in Table 6.

< **Please insert Table 6 Total first order hyperpolarizability βCT calculated by solvatochromic and computed method for TPA BIZ and TPA BTZ>**

The difference in the experimental and computed values of β_{xxx} for TPA BIZ and TPA BTZ are in order of (x 10^{-30}) esu. The trends across the non-polar to polar solvents is well described by the computational methods. Polar solvents show higher β_{xxx} values and these are reflected both in computational methods. The compound TPA BIZ has calculated values of 26 (× 10^{-30}) esu to 41 (× 10^{-30}) esu and experimental values from 20 (× 10^{-30}) esu to 24 (× 10^{-30}) esu across the solvents. The compound TPA BTZ has calculated values of 59 (× 10^{-30}) esu to 88 (× 10^{-30}) esu and experimental values from 32 (× 10^{-30}) esu to 41 (× 10^{-30}) esu across the solvents. The value of β_0 or total first order hyperpolarizability of the molecule gives an estimate of the NLO properties of the organic molecules. This value considers all the directional tensor components of hyperpolarizability. The computed values were compared with the values obtained for urea. As urea is one of the exemplary molecules used in the study of the NLO properties of molecular systems, it is used often as a threshold value for virtual purpose of comparison. The total hyperpolarizability calculated is 70-110 times and 159-238 times greater than that of urea (0.37×10^{-30} esu) in case

of TPA BIZ and TPA BTZ. The effect of the substitution of benzothiazole ring system as against benzimidazole is clear and shows a higher first order hyperpolarizability. The solvent effect is consistently shows higher value in polar solvents by computational method.

Calculation of solvatochromic descriptor of γ_{SD} from the solvatochromic data

The second-order (or cubic) hyperpolarizability at molecular level originating from the electronic polarization in the non-resonant region can be treated by a three-level model [21,22,85–87]. The quasi-two level model in place of the three level model using the density matrix formalism to a simpler expression [88–90].

$$< \gamma > \propto \frac{1}{E_{eg}^3} \mu_{eg}^2 \left(\Delta\mu^2 - \Delta\mu_{eg}^2\right) \ldots\ldots\ldots (9)$$

The value

$$\frac{1}{E_{eg}^3} \mu_{eg}^2 \left(\Delta\mu^2 - \Delta\mu_{eg}^2\right) (10)$$

< **Please insert Table 7 Second order static hyperpolarizability obtained by solvatochromic and computational method** >

The second order hyperpolarizability can be expressed as the ‘‘solvatochromic descriptor” and the values calculated are given in Table 7. The solvatochromic descriptor ($\bar{\gamma}$) of second order hyperpolarizability of compounds show higher values in case of a benzothiazole ring containing molecules than benzimidazole containing molecules. This can be understood on the basis of higher electron pulling effect of benzothiazole ring as compared to benzimidazole ring system, which helps in creating a stronger dipole and contribute to the hyperpolarizabilities. Like β_{xxx} and β_0 the solvatochromic descriptor is also affected by the polarity of solvent. The solvent effect is also observed on this parameter, higher the polarity of the solvent, higher the second order hyperpolarizability. The compound TPA BIZ has calculated values of 280 ($\times 10^{-36}$) esu to 426 ($\times 10^{-30}$) esu and experimental values from 9 ($\times 10^{-36}$) esu to 10 ($\times 10^{-36}$) esu. The compound TPA BTZ has calculated values of 446 ($\times 10^{-36}$) esu to 540 ($\times 10^{-36}$) esu and experimental values from 27 ($\times 10^{-36}$) esu to 31 ($\times 10^{-36}$) esu. The second order hyperpolarizability calculated is 412-626 times and 493-778 times greater than that of urea ($\gamma_{urea} = 0.68 \times 10^{-36}$ esu) in case of TPA BIZ and

TPA BTZ. The individual components of the second order static hyperpolarizability γ were obtained computationally. The values are considered to be proportional to the solvatochromic descriptor γ of the second order hyperpolarizability. The values show a trend where higher polarity solvents show higher values of γ and a similar trend is followed by the solvatochromically obtained values.

Non-linear optical properties TPA BIZ and TPA BTZ dyes using DFT and TD-DFT method

The static first hyperpolarizability (β_o) and its related properties (μ, α_0, $\Delta\alpha$, β, γ) for TPA BIZ and TPA BTZ dyes were calculated using the B3LYP, CAM-B3LYP and BHHLYP functionals with 6-311+G(d,p) basis set on the basis of the finite-field approach [91]. In the presence of an applied field, the energy of the system is a function of the electric field, and the hyperpolarizability is a rank three tensor that can be described by a 3 × 3 × 3 matrix. The 27 components of three-dimensional matrix can be reduced to 10 components due to Kleinman symmetry [92]. The matrix can be given in the lower tetrahedral format. It is obvious that the lower part of the 3 × 3 × 3 matrices is tetrahedral. The components of β are defined as the coefficient in the Taylor series expansion of the energy in the external electric field. When the external electric field is weak and homogeneous, this expansion becomes

$$E = E^0 - \mu_\alpha f_\alpha - \frac{1}{2\alpha_{\alpha\beta}F_\alpha F_\beta} - f\frac{1}{6\beta_{\alpha\beta\gamma}F_\alpha F_\beta F_\gamma} \ldots\ldots (11)$$

Where E° is the energy of the unperturbed molecules,
F_α is the field at the origin,
μ_α, $\alpha_{\alpha\beta}$ and $\beta_\alpha\beta_\gamma$ are the components of dipole moment ,polarizability and the first hyperpolarizabilities respectively. The complete equations for calculating the magnitude of total static dipole moment (μ), the mean polarizability (α_0), the anisotropy of the polarizability ($\Delta\alpha$), the mean first hyperpolarizability (β) and static second hyperpolarizability (γ) using the *x*, *y*, z components from Gaussian 09W output are defined as follows [53]:

$$\mu = (\mu_x^2 + \mu_y^2 + \mu_z^2)^{1/2} \quad (12)$$

$$\alpha_0 = (1/3)\ \alpha_{xx} + \alpha_{yy} + \alpha_{zz} \quad (13)$$

$$\Delta\alpha = 2^{-1/2}\ [(\alpha_{xx} - \alpha_{yy})^2 + (\alpha_{yy} - \alpha_{zz})^2 + (\alpha_{zz} - \alpha_{xx})^2 + 6\alpha^2_{xx}]^{1/2} \quad (14)$$

$$\beta_{total} = [(\beta_{xxx} + \beta_{xyy} + \beta_{xzz})^2 + (\beta_{yyy} + \beta_{xxy} + \beta_{yzz})^2 + (\beta_{zzz} + \beta_{xxz} + \beta_{yyz})^2] \quad (15)$$

$$\bar{\gamma} = (1/5)\ [(\gamma_{xxxx} + \gamma_{yyyy} + \gamma_{zzzz} + 2\gamma_{xxyy} + 2\gamma_{yyzz} + 2\gamma_{zzxx})] \quad (16)$$

The values calculated for total static dipole moment (μ), the mean polarizability (α_0), the anisotropy of the polarizability ($\Delta\alpha$), the mean first hyperpolarizability (β) and static second hyperpolarizability (γ), of the TPA BIZ and TPA BTZ dyes in different solvent environments using Equations (12-16), respectively, are enlisted in Tables 5-7and Supporting Information 533 (SI) tables S6-S11. A comparison of the B3LYP, CAM-B3LYP and BHHLYP hyperpolarizabilities suggests that the results obtained using the B3LYP functional might be overestimating the hyperpolarizability values. This conclusion is based on benchmark studies [93–95] in which CAM-B3LYP was found to perform much better than B3LYP for nonlinear optical properties based on comparison with highly accurate coupled-cluster models pointed out by Hammond and Kowalski [96].

Vibrational contribution to the linear and NLO response:

In push-pull chromophores, vibrations are generally strongly coupled with conjugated electrons in the system. Hence along with the electronic transitions the vibrational transitions play vital role in determining the NLO properties. The coupling between the electronic polarization and vibration leads to a considerable vibrational contribution to the overall NLO response [97] .In this context, DFT is a good computational tool to study the vibrational contribution to polarizability and hyperpolarizabilities of NLO chromophores [98,99]. We have obtained the vibrational contributions to static electronic polarizability and hyperpolarizabilities using B3LYP functional with 6-311+G(d,p) basis set in two solvents. **Table-8** presents the DFT results of the

diagonal electronic and vibrational contributions to the linear polarizability (α) and first hyperpolarizability (β).

< **Please insert Table 8 Diagonal electronic and vibrational contributions to dipole polarizabilities and first hyperpolarizabilities of TPA BIZ and TPA BTZ obtained from of B3LYP/6-311+G(d,p) calculations in various solvent. (All values are in a.u.)>**

Table-8 shows that along with electronic part there is substantial contribution of vibrational part to the polarizability and hyperpolarizability. For TPA BIZ and TPA BTZ the ratios of vibrational to electronic contribution in polarizability ($\alpha^v/\alpha^{e)}$ are 0.451 to 0.557 and 0.313 to 0.401 in toluene (nonpolar) and ethanol (polar with hydrogen bonding effect) respectively. In case of first hyperpolarizability the ratios of vibrational to electronic contribution ($\beta^v/\beta^{e)}$ are -1.239 to -1.061 and -0.040 to 0.003 in toluene and ethanol respectively. This confirms that the vibrational motions play crucial role in determining the NLO properties of these dyes particularly in solvent environments wherein solvation is likely to affect the vibrations.

Fundamental limits for the first and second order hyperpolarizability values

The fundamental limits of NLO response for the TPA BIZ and TPA BTZ Push-pull chromophores can be obtained by the limiting theory proposed by Kuzyk [100,101]. It is the sum-rule-restricted (SR) three-level model which produce a two-level-limit (2L) for β (β_{2L}^{*SR} or βmax) depends exclusively on the conjugated π electrons N from double or triple bond and the transition energy E_{10} between the ground and first excited state, obtained from λmax absorption. The limit for β* is obtained from eq.17 in different solvents using their respective refractive indexes (n) of respective solvent.

$$\beta_{2L}^{*SR} \leq \sqrt[4]{3}\left(\frac{n^2+2}{3}\right)^3\left(\frac{e\hbar}{\sqrt{m}}\right)^3\frac{N^{3/2}}{E_{10}^{7/2}} \qquad (17)$$

e and *m* are the charge and mass of electron. $\hbar = h/2\pi$.

Similarly limit for the second order hyperpolarizability (γ) can be estimated by eq. 18[102,103]. The γ values have two possible fundamental limits for i.e. negative limit which is for a centrosymmetric molecule and positive limit for an asymmetric molecule.

$$-\frac{e^4\hbar^4}{m^2}\left(\frac{N^2}{E_{10}^5}\right) \leq \gamma \leq 4\frac{e^4\hbar^4}{m^2}\left(\frac{N^2}{E_{10}^5}\right) \quad (18)$$

The limiting values for β and γ obtained from eq. 17 and 18 are compared with the corresponding values obtained by solvatochromic and computational methods for TPA BIZ and TPA BTZ in table 9.

< **Please insert Table 9 Comparison of solvatochromic and theoretical values with the limiting values of hyperpolarizability for TPA BIZ and TPA BTZ>**

Table 9 shows that for TPA BIZ and TPA BTZ in all solvents the β values below the βmax limit and γ values are within the estimated limiting values.

Conclusions

In summary, NLO properties of triphenylamine-based dyes TPA BIZ and TPA BTZ were studied using the solvatochromic method and the solvent dependent shift in the emission wavelength is observed. Furthermore DFT and TD-DFT computations were performed to estimate the NLO properties of triphenylamine-based dyes TPA BIZ and TPA BTZ using the B3LYP functional (in the ground- and excited-state geometries) and the CAM-B3LYP and BHHLYP functionals (in the ground-state geometry only). The theoretical examination on non-linear optical properties was performed on the key parameters of polarizability and hyperpolarizability. A remarkable increase in non-linear optical response is observed on insertion of benzothiazole unit compared to benzimidazole unit. Triphenylamine-based dyes TPA BIZ and TPA BTZ can act as a promising organic NLO material for optoelectronic devices.

Acknowledgments SK is thankful to UGC for giving study leave (FIP) and SIES College for sanctioning the study leave. PR and LR acknowledge facilities from the University of Mauritius. IAA and PR extend their appreciation to the International Scientific Partnership Program ISPP at King Saud University for funding this research work through ISPP# 0070.

References

[1] D.R. Kanis, M.A. Ratner, T.J. Marks, Design and Construction of Molecular Assemblies with Large Second-Order Optical Nonlinearities . Quantum Chemical Aspects, Chem. Phys. Lett. 94 (1994) 195–242. doi:0009-2665194lO794-0195.

[2] D.M. Burland, R.D. Miller, C. a Walsh, Second-order nonlinearity in poled-polymer systems, Chem. Rev. 94 (1994) 31–75. doi:10.1021/cr00025a002.

[3] S.R. Marder, B. Kippelen, A.K.-Y. Jen, N. Peyghambarian, Design and synthesis of chromophores and polymers for electro-optic and photorefractive applications, Nature. 388 (1997) 845–851. doi:10.1038/42190.

[4] G. Koeckelberghs, M. Vangheluwe, I. Picard, L. De Groof, T. Verbiest, A. Persoons, C. Samyn, Synthesis and properties of new chiral donor-embedded polybinaphthalenes for nonlinear optical applications, Macromolecules. 37 (2004) 8530–8537. doi:10.1021/ma0491816.

[5] H. Bin Li, J.Z. Zhang, J. Zhang, Y. Wu, Y.A. Duan, Z.M. Su, Y. Geng, Theoretical studies on organic D-π-A sensitizers with planar triphenylamine donor and different π-linkers for dyes-sensitized solar cells, J. Mol. Model. 20 (2014) 1–12. doi:10.1007/s00894-014-2309-2.

[6] D. Cvejn, E. Michail, I. Polyzos, N. Almonasy, O. Pytela, M. Klikar, T. Mikysek, V. Giannetas, M. Fakis, F. Bures, Modulation of (non)linear optical properties in tripodal molecules by variation of the peripheral cyano acceptor moieties and the pi-spacer, J. Mater. Chem. C. 3 (2015) 7345–7355. doi:10.1039/c5tc01293g.

[7] L.R. Dalton, P. a. Sullivan, D.H. Bale, Electric field poled organic electro-optic materials: State of the art and future prospects, Chem. Rev. 110 (2010) 25–55. doi:10.1021/cr9000429.

[8] V. Crasta, V. Ravindrachary, S. Lakshmi, S.N. Pramod, M. a. Shridar, J. Shashidhara Prasad, Growth, characterization and crystal structure analysis of 1-(4-chlorophenyl)-3-(4-chlorophenyl)-2-propen-1-one, J. Cryst. Growth. 275 (2005) 329–335. doi:10.1016/j.jcrysgro.2004.10.110.

[9] D. Cvejn, S. Achelle, O. Pytela, J.P. Malval, A. Spangenberg, N. Cabon, F. Bures, F. Robin-Le Guen, Tripodal molecules with triphenylamine core, diazine peripheral groups and extended π conjugated linkers, Dye. Pigment. 124 (2016) 101–109. doi:10.1016/j.dyepig.2015.09.012.

[10] A.B.H.R. LARRY R. DALTON*, AARON W. HARPER*, The role of London forces in defining noncentrosymmetric order of High Dipole Moment – High Hyperpolarizability Chromophores in electrically poled polymeric thin films, Proc. Natl. Acad. Sci. 94 (1997) 4842–4847. doi:0027-8424/97/944842.

[11] L. Shi, M. Horn, S. Kobayashi, H. Mayr, Carbocationic n-endo-trig cyclizations, Chem. - A Eur. J. 15 (2009) 8533–8541. doi:10.1002/chem.200901246.

[12] P.R. Varanasi, A.K. Jen, J. Chandrasekhar, I.N.N. Namboothiri, A. Rathna, The Important Role of Heteroaromatics in the Design of Efficient Second-Order Nonlinear Optical Molecules : Theoretical Investigation on Push - Pull Heteroaromatic Stilbenes, J. Am.

Chem. Soc. 7863 (1996) 12443–12448. doi:S0002-7863(96)00136-9.

[13] I.D.L. Albert, T.J. Marks, M. a. Ratner, Large molecular hyperpolarizabilities. Quantitative analysis of aromaticity and auxiliary donor-acceptor effects, J. Am. Chem. Soc. 119 (1997) 6575–6582. doi:10.1021/ja962968u.

[14] H. Kang, A. Facchetti, P. Zhu, H. Jiang, Y. Yang, E. Cariati, S. Righetto, R. Ugo, C. Zuccaccia, A. Macchioni, C.L. Stern, Z. Liu, S.T. Ho, T.J. Marks, Exceptional molecular hyperpolarizabilities in twisted ??-electron system chromophores, Angew. Chemie - Int. Ed. 44 (2005) 7922–7925. doi:10.1002/anie.200501581.

[15] H. Kang, A. Facchetti, H. Jiang, E. Cariati, S. Righetto, R. Ugo, C. Zuccaccia, A. Macchioni, C.L. Stern, Z. Liu, S.T. Ho, E.C. Brown, M. a. Ratner, T.J. Marks, Ultralarge hyperpolarizability twisted π-electron system electro-optic chromophores: Synthesis, solid-state and solution-phase structural characteristics, electronic structures, linear and nonlinear optical properties, and computational studies, J. Am. Chem. Soc. 129 (2007) 3267–3286. doi:10.1021/ja0674690.

[16] J.S. Yang, K.L. Liau, C.Y. Li, M.Y. Chen, Meta conjugation effect on the torsional motion of aminostilbenes in the photoinduced intramolecular charge-transfer state, J. Am. Chem. Soc. 129 (2007) 13183–13192. doi:10.1021/ja0741022.

[17] G. Meshulam, Z. Kotler, G. Berkovic, Time-resolved electric-field-induced second harmonic: simultaneous measurement of first and second molecular hyperpolarizabilities., Opt. Lett. 27 (2002) 1132–1134. doi:10.1364/OL.27.001132.

[18] G.J.T. Heesink, a G.T. Ruiter, N.F. van Hulst, B. Bolger, Determination of hyperpolarizability tensor components by depoarized hyper rayleigh scattering, Phys. Rev. Lett. 71 (1993) 999. doi:0031 -9007/93/71 (7)/999.

[19] M. S. Paley and J. M. Harris, A Solvatochromic Method for Determining Second-Order Polarizabilities of Organic Molecules, J. Org. Chem. 54 (1989) 3174–3178. doi:0022-3263/89/1954-3774.

[20] B. Carlotti, R. Flamini, I. Kikaš, U. Mazzucato, a. Spalletti, Intramolecular charge transfer, solvatochromism and hyperpolarizability of compounds bearing ethenylene or ethynylene bridges, Chem. Phys. 407 (2012) 9–19. doi:10.1016/j.chemphys.2012.08.006.

[21] O. Kwon, M. Jazbinsek, J. Seo, P. Kim, E. Choi, Y. Sup, P. Günter, First hyperpolarizability orientation in asymmetric pyrrole-based polyene chromophores, Dye. Pigment. 85 (2010) 162–170. doi:10.1016/j.dyepig.2009.10.019.

[22] J.L. Oudar, D.S. Chemla, Hyperpolarizabilities of the nitroanilines and their relations to the excited state dipole moment, J. Chem. Phys. 66 (1977) 2664–2668. doi:10.1063/1.434213.

[23] F. Castet, A. Pic, B. Champagne, Linear and nonlinear optical properties of arylvinyldiazine dyes: A theoretical investigation, Dye. Pigment. 110 (2014) 256–260. doi:10.1016/j.dyepig.2014.03.021.

[24] P.S. Liyanage, R.M. De Silva, K.M.N. De Silva, Nonlinear optical (NLO) properties of novel organometallic complexes: High accuracy density functional theory (DFT) calculations, J. Mol. Struct. THEOCHEM. 639 (2003) 195–201.

686 doi:10.1016/j.theochem.2003.08.009.

687 [25] D. V. Petrov, W.M. Faustino, Hyper-Rayleigh scattering in p-nitroaniline with excited
688 states obtained by 355 nm optical pump, Opt. Commun. 203 (2002) 145–150.
689 doi:10.1016/S0030-4018(01)01738-2.

690 [26] W.M. Faustino, D. V Petrov, First hyperpolarizability of the molecular excited states :
691 Calculations for p -nitroaniline and comparison with experiments, Chem. Phys. Lett. 365
692 (2002) 170–175. doi:10.1016/S0009-2614(02)01429-X.

693 [27] J. Cremer, C. a Briehn, Novel Highly Fluorescent Triphenylamine-Based
694 Oligothiophenes, Chem. Mater. 19 (2007) 4155–4165. doi:doi:10.1021/cm0700448.

695 [28] U. Mitschke, P. Bäuerle, The electroluminescence of organic materials, J. Mater. Chem.
696 10 (2000) 1471–1507. doi:10.1039/a908713c.

697 [29] C.D. Dimitrakopoulos, P.R.L. Malenfant, Organic thin film transistors for large area
698 electronics, Adv. Mater. 14 (2002) 99–117. doi:10.1002/1521-4095(20020116)14.

699 [30] N. Satoh, T. Nakashima, K. Yamamoto, Metal-Assembling Dendrimers with a
700 Triarylamine Core and Their Application to a Dye-Sensitized Solar Cell, J. Am. Chem.
701 Soc. 127 (2005) 13030–13038. doi:10.1021/ja050765c.

702 [31] P. Hrob, V. Hrob, I. Sigmundov, I. Polyzos, P. Persephonis, Benzothiazoles with Tunable
703 Electron-Withdrawing Strength and Reverse Polarity : A Route to Triphenylamine-Based
704 Chromophores with Enhanced Two-Photon Absorption, J. Org. Chem. 76 (2011) 8726–
705 8736. doi:org/10.1021/jo201411t.

706 [32] F. Gao, J. Liu, L. Yang, Q. Wang, H. Li, S. Zhang, Synthesis and spectral tuning of novel
707 triphenylamine-based derivatives containing electron donor-acceptor groups, Chinese J.
708 Chem. 28 (2010) 950–960. doi:10.1002/cjoc.201090177.

709 [33] Y. Yang, F. Liu, H. Wang, S. Bo, J. Liu, L. Qiu, Triarylaminophenyl-Based
710 Chromophores By Introducing Heteroatoms To the Donor, J. Mater. Chem. C. 3 (2015)
711 5297–5306. doi:10.1039/C5TC00723B.

712 [34] L. Kong, J. Yang, H. Zhou, S. Li, F. Hao, Q. Zhang, Y. Tu, J. Wu, Z. Xue, Y. Tian,
713 Synthesis, photophysical properties and TD-DFT calculation of four two-photon
714 absorbing triphenylamine derivatives, Sci. China Chem. 56 (2013) 106–116.
715 doi:10.1007/s11426-012-4794-4.

716 [35] A. Mahmood, S.U. Khan, U. Ali, M. Ramzan, S. Ashraf, M. Hussain, Effect of thiophene
717 rings on UV / visible spectra and non-linear optical (NLO) properties of triphenylamine
718 based dyes : a quantum chemical perspective, J. Chem. Phys. 74 (2015) 418–422.
719 doi:10.1002/poc.3427.

720 [36] K. Srinivas, G. Sivakumar, C. Ramesh, M.A. Reddy, K. Bhanuprakash, V.J. Rao, C.
721 Chen, Y. Hsu, J.T. Lin, Novel 1 , 3 , 4-oxadiazole derivatives as efficient sensitizers for
722 dye-sensitized solar cells : A combined experimental and computational study, Synth.
723 Met. 161 (2011) 1671–1681. doi:10.1016/j.synthmet.2011.06.001.

724 [37] W. Li, Q. Li, C. Duan, S. Liu, L. Ying, F. Huang, Y. Cao, Design and synthesis of star-
725 burst triphenyamine-based pi-conjugated molecules, Dye. Pigment. 113 (2015) 1–7.
726 doi:10.1016/j.dyepig.2014.07.034.

[38] C. Lambert, W. Gaschler, E. Schmälzlin, K. Meerholz, C. Bräuchle, Subchromophore interactions in tricyanovinyl-substituted triarylamines—a combined experimental and computational study, J. Chem. Soc. Perkin Trans. 2. (1999) 577–588. doi:10.1039/a808009g.

[39] R. Lartia, C. Allain, G. Bordeau, F. Schmidt, C. Fiorini-Debuisschert, F. Charra, M.P. Teulade-Fichou, Synthetic strategies to derivatizable triphenylamines displaying high two-photon absorption, J. Org. Chem. 73 (2008) 1732–1744. doi:10.1021/jo702002y.

[40] L. Zhou, C. Jia, Z. Wan, Z. Li, J. Bai, L. Zhang, J. Zhang, X. Yao, Triphenylamine-based organic dyes containing benzimidazole derivatives for dye-sensitized solar cells, Dye. Pigment. 95 (2012) 743–750. doi:10.1016/j.dyepig.2012.05.007.

[41] Y. Yang, B. Li, L. Zhang, Y. Guan, Triphenylamine based benzimidazole and benzothiazole : Synthesis and applications in fl uorescent chemosensors and laser dyes, J. ofLuminescence. 145 (2014) 895–898. doi:10.1016/j.jlumin.2013.09.008.

[42] O. Treutler, R. Ahlrichs, Efficient molecular numerical integration schemes, J. Chem. Phys. 102 (1995) 346–353. doi:10.1063/1.469408.

[43] C. Lee, W. Yang, R.G. Parr, Development of the Colle-Salvetti correlation-energy formula into a functional of the electron density, Phys. Rev. B. 37 (1988) 785–789. doi:10.1103/PhysRevB.37.785.

[44] A.D. Becke, Density-functional thermochemistry. III. The role of exact exchange, J. Chem. Phys. 98 (1993) 5648–5652. doi:10.1063/1.464913.

[45] B. Champagne, E. Botek, M. Nakano, T. Nitta, K. Yamaguchi, Basis set and electron correlation effects on the polarizability and second hyperpolarizability of model open-shell π -conjugated systems, J. Chem. Phys. 122 (2005) 114315. doi:10.1063/1.1880992.

[46] A.D. Becke, A new mixing of Hartree–Fock and local density-functional theories, J. Chem. Phys. 98 (1993) 1372–1377. doi:org/10.1063/1.464304.

[47] T. Yanai, D.P. Tew, N.C. Handy, A new hybrid exchange – correlation functional using the, Chem. Phys. Lett. 393 (2004) 51–57. doi:10.1016/j.cplett.2004.06.011.

[48] R. Ditchfield, Self-Consistent Molecular-Orbital Methods. IX. An Extended Gaussian-Type Basis for Molecular-Orbital Studies of Organic Molecules, J. Chem. Phys. 54 (1971) 724. doi:10.1063/1.1674902.

[49] R. Krishnan, H.B. Schlegel, J. a Pople, Derivative studies in configuration-interaction theory, J. Chem. Phys. 72 (1980) 4654–4655. doi:10.1063/1.439708.

[50] J.E. Barnsley, G.E. Shillito, C.B. Larsen, H. Van Der Salm, L.E. Wang, N.T. Lucas, K.C. Gordon, Benzo[c][1,2,5]thiadiazole Donor − Acceptor Dyes: A Synthetic, Spectroscopic, and Computational Study, J. Phys. Chem. A. 120 (2016) 1853–1866. doi:10.1021/acs.jpca.6b00447.

[51] M. Cossi, V. Barone, R. Cammi, J. Tomasi, Ab initio study of solvated molecules: a new implementation of the polarizable continuum model, Chem. Phys. Lett. 255 (1996) 327–335. doi:10.1016/0009-2614(96)00349-1.

[52] J. Tomasi, B. Mennucci, R. Cammi, Quantum mechanical continuum solvation models,

Chem. Rev. 105 (2005) 2999–3093. doi:10.1021/cr9904009.

[53] C. Meganathan, S. Sebastian, M. Kurt, K.W. Lee, N. Sundaraganesan, Molecular structure, spectroscopic (FTIR, FTIR gas phase, FT-Raman) first-order hyperpolarizability and HOMO-LUMO analysis of 4-methoxy-2-methyl benzoic acid, J. Raman Spectrosc. 41 (2010) 1369–1378. doi:10.1002/jrs.2562.

[54] J. Frisch, M. J.; Trucks, G.W.; Schlegel, H. B.; Scuseria, G. E.; Robb, M. A.; Cheeseman, H.. C. R.; Scalmani, G.; Barone, V.; Mennucci, B.; Petersson, G. A.; Nakatsuji, J.L.. M.; Li, X.; Hratchian, H. P.; Izmaylov, A. F.; Bloino, J.; Zheng, G.; Sonnenberg, T.. Hada, M.; Ehara, M.; Toyota, K.; Fukuda, R.; Hasegawa, J.; Ishida, M.; Nakajima, J.E.. Honda, Y.; Kitao, O.; Nakai, H.; Vreven, T.; Montgomery, J. A., Jr.; Peralta, V.N.. Ogliaro, F.; Bearpark, M.; Heyd, J. J.; Brothers, E.; Kudin, K. N.; Staroverov, S.S.. Kobayashi, R.;Normand, J.; Raghavachari, K.; Rendell, A.; Burant, J. C.; Iyengar, J.B.. B. Tomasi, J.; Cossi, M.;Rega, N.; Millam, N. J.; Klene, M.;Knox, J. E.; Cross, A.J.. V.; Adamo, C.; Jaramillo, J.; Gomperts, R.; Stratmann, R. E.; Yazyev, O.; Austin, V. Cammi, R.; Pomelli, C.; Ochterski, J.W.;Martin, R. L.; Morokuma, K.; Zakrzewski, O.. G.; Voth, G. A.; Salvador, P.; Dannenberg, J. J.; Dapprich, S.; Daniels, A. D.; Farkas, D.J. Foresman, J. B.; Ortiz, J. V.; Cioslowski, J.; Fox, Gaussian 09, Revision C.01, (2010).

[55] R. Dooley, K. Milfeld, C. Guiang, S. Pamidighantam, G. Allen, From proposal to production: Lessons learned developing the computational chemistry Grid cyberinfrastructure, J. Grid Comput. 4 (2006) 195–208. doi:10.1007/s10723-006-9043-7.

[56] J.G. Kent Milfeld and Chona Guiang, Sudhakar Pamidighantam, Cluster Computing through an Application-Oriented Computational Chemistry Grid., Proc. 2005 Linux Clust. HPC Revolut. . (2005).

[57] R. Dooley, G. Allen, S. Pamidighantam, Computational Chemistry Grid: Production cyberinfrastructure for computational chemistry, in: Proc. 13th Annu. Mardi Gras Conf., 2005: p. 83.

[58] Przemysław Krawczyk, DFT study of linear and nonlinear optical properties of donor-acceptor substituted stilbenes , azobenzenes and benzilideneanilines, J. Mol. Model. 16 (2010) 659–668. doi:10.1007/s00894-009-0623-x.

[59] A.P. Kulkarni, Y. Zhu, A. Babel, P. Wu, S.A. Jenekhe, New Ambipolar Organic Semiconductors. 2. Effects of Electron Acceptor Strength on Intramolecular Charge Transfer Photophysics, Highly Efficient Electroluminescence, and Field-Effect Charge Transport of Phenoxazine-Based Donor−Acceptor Materials, Chem. Mater. 20 (2008) 4212–4223. doi:10.1021/cm7022136.

[60] Y. Zheng, A.S. Batsanov, V. Jankus, F.B. Dias, M.R. Bryce, A.P. Monkman, Bipolar molecules with high triplet energies: Synthesis, photophysical, and structural properties, J. Org. Chem. 76 (2011) 8300–8310. doi:10.1021/jo201488v.

[61] K.C. Moss, K.N. Bourdakos, V. Bhalla, K.T. Kamtekar, M.R. Bryce, M.A. Fox, H.L. Vaughan, F.B. Dias, A.P. Monkman, Tuning the intramolecular charge transfer emission from deep blue to green in ambipolar systems based on dibenzothiophene S, S -dioxide by manipulation of conjugation and strength of the electron donor units, J. Org. Chem. 75 (2010) 6771–6781. doi:10.1021/jo100898a.

[62] M.E. Reish, A.J. Kay, A. Teshome, I. Asselberghs, K. Clays, K.C. Gordon, Testing Computational Models of Hyperpolarizability in a Merocyanine Dye Using Spectroscopic and DFT Methods, J. Phys. Chem. A. 116 (2012). doi:10.1021/jp301455r.

[63] S. Jeong, M.K. Kim, S.H. Kim, J.I. Hong, Efficient deep-blue emitters based on triphenylamine-linked benzimidazole derivatives for nondoped fluorescent organic light-emitting diodes, Org. Electron. Physics, Mater. Appl. 14 (2013) 2497–2504. doi:10.1016/j.orgel.2013.06.022.

[64] S. Gong, Y. Zhao, M. Wang, C. Yang, C. Zhong, J. Qin, D. Ma, Versatile benzimidazole/triphenylamine hybrids: Efficient nondoped deep-blue electroluminescence and good host materials for phosphorescent emitters, Chem. - An Asian J. 5 (2010) 2093–2099. doi:10.1002/asia.201000206.

[65] D. Sajan, Y. Erdogdu, T. Kuruvilla, I.H. Joe, Vibrational spectra and first-order molecular hyperpolarizabilities of p-hydroxybenzaldehyde dimer, J. Mol. Struct. 983 (2010) 12–21. doi:10.1016/j.molstruc.2010.08.003.

[66] Y. Dwivedi, G. Tamashiro, L. De Boni, S.C. Zilio, Nonlinear optical characterizations of dibenzoylmethane in solution, Opt. Commun. 293 (2013) 119–124. doi:10.1016/j.optcom.2012.11.065.

[67] Z. Ge, T. Hayakawa, S. Ando, M. Ueda, T. Akiike, H. Miyamoto, T. Kajita, M. Kakimoto, Solution-Processible Bipolar Triphenylamine-Benzimidazole Derivatives for Highly Efficient Single-Layer Organic Light-Emitting Diodes, Chem. Mater. 20 (2008) 2532–2537. doi:10.1021/cm7035458.

[68] G. Angulo, J. Dobkowski, A. Kapturkiewicz, K. MacIolek, Photophysics and electrochemistry of quinoxaline chromophores decorated with thiophene or furane subunits, J. Photochem. Photobiol. A Chem. 213 (2010) 101–106. doi:10.1016/j.jphotochem.2010.05.007.

[69] A.P. Kulkarni, P. Wu, T.W. Kwon, S.A. Jenekhe, Phenothiazine-Phenylquinoline Donor - Acceptor Molecules : Effects of Structural Isomerism on Charge Transfer Photophysics and Electroluminescence, J. Phys. Chem. B. 109 (2005) 19584–19594. doi:DOI: 10.1021/jp0529772.

[70] S. Muthu, M. Prasath, E.I. Paulraj, R.A. Balaji, Spectrochimica Acta Part A : Molecular and Biomolecular Spectroscopy FT-IR , FT-Raman spectra and ab initio HF and DFT calculations, Spectrochim. Acta Part A Mol. Biomol. Spectrosc. 120 (2014) 185–194. doi:10.1016/j.saa.2013.09.150.

[71] R.G. Pearson, Chemical hardness and density functional theory, J. Chem. Sci. 117 (2005) 369–377. doi:10.1007/BF02708340.

[72] E.M. Breitung, C.F. Shu, R.J. McMahon, Thiazole and thiophene analogues of donor-acceptor stilbenes: Molecular hyperpolarizabilities and structure-property relationships, J. Am. Chem. Soc. 122 (2000) 1154–1160. doi:10.1021/ja9930364.

[73] R.J. Cave, M.D. Newton, Generalization of the Mulliken-Hush treatment for the calculation of electron transfer matrix elements, Chem. Phys. Lett. 249 (1996) 15–19. doi:10.1016/0009-2614(95)01310-5.

[74] R.J. Cave, M.D. Newton, Calculation of electronic coupling matrix elements for ground and excited state electron transfer reactions: Comparison of the generalized Mulliken–Hush and block diagonalization methods, J. Chem. Phys. 106 (1997) 9213. doi:10.1063/1.474023.

[75] C. Creutz, M.D. Newton, N. Sutin, Metal—lingad and metal—metal coupling elements, J. Photochem. Photobiol. A Chem. 82 (1994) 47–59. doi:10.1016/1010-6030(94)02013-2.

[76] D. Beljonne, G. Pourtois, M.A. Ratner, J.L. Brédas, Pathways for Photoinduced Charge Separation in DNA Hairpins, J. Am. Chem. Soc. 125 (2003) 14510–14517. doi:10.1021/ja035596f.

[77] J. Lappe, R.J. Cave, M.D. Newton, I. V. Rostov, A theoretical investigation of charge transfer in several substituted acridinium ions, J. Phys. Chem. B. 109 (2005) 6610–6619. doi:10.1021/jp0456133.

[78] J. Zheng, Y.K. Kang, M.J. Therien, D.N. Beratan, Generalized Mulliken−Hush Analysis of Electronic Coupling Interactions in Compressed π-Stacked Porphyrin−Bridge−Quinone Systems, J. Am. Chem. Soc. 127 (2005) 11303–11310. doi:10.1021/ja050984y.

[79] A. Abbotto, L. Beverina, S. Bradamante, A. Facchetti, C. Klein, G. a. Pagani, M. Redi-abshiro, R. Wortmann, A distinctive example of the cooperative interplay of structure and environment in tuning of intramolecular charge transfer in second-order nonlinear optical chromophores, Chem. - A Eur. J. 9 (2003) 1991–2007. doi:10.1002/chem.200204356.

[80] F. Momicchioli, G. Ponterini, D. Vanossi, First- and Second-Order Polarizabilities of Simple Merocyanines. An Experimental and Theoretical Reassessment of the Two-Level Model, J. Phys. Chem. A. 112 (2008) 11861–11872. doi:10.1021/jp8080854.

[81] E. Benassi, F. Egidi, V. Barone, General Strategy for Computing Nonlinear Optical Properties of Large Neutral and Cationic Organic Chromophores in Solution, J. Phys. Chem. B. 119 (2015) 3155. doi:10.1021/jp512342y.

[82] F. Egidi, T. Giovannini, M. Piccardo, J. Bloino, Europe PMC Funders Group Stereo-electronic , vibrational , and environmental contributions to polarizabilities of large molecular systems : a feasible anharmonic protocol, J Chem Theory Comput. 10 (2015) 2456–2464. doi:10.1021/ct500210z.Stereo-electronic.

[83] E.G. McRae, Theory of Solvent Effects on Molecular Electronic Spectra. Frequency Shifts, J. Phys. Chem. 61 (1954) 1957. doi:10.1021/j150551a012.

[84] S. Bruni, E. Cariati, F. Cariati, F.A. Porta, S. Quici, D. Roberto, Determination of the quadratic hyperpolarizability of trans-4-[4-(dimethylamino)styryl]pyridine and 5-dimethylamino-1,10-phenanthroline from solvatochromism of absorption and fluorescence spectra: A comparison with the electric-field-induced second-harmon, Spectrochim. Acta - Part A Mol. Biomol. Spectrosc. 57 (2001) 1417–1426. doi:10.1016/S1386-1425(00)00483-2.

[85] L. Cbeng, W. Tam, S.H. Stevenson, G.R. Meredith, S.R. Marder, Experimental Investigations of Organic Molecular Nonlinear Optical Polarizabilities . 1 . Methods and Results on Benzene and Stilbene Derivatives, J. Phys. Chem. 95 (1991) 10631–10643. doi:0022-3654/91/2095-10631.

[86] M. Yamashita, S. Kikuma, Y. Yamaoka, H. Murakami, R. Morita, H. Shigekawa, Nonresonant femtosecond second hyperpolarizabilities of intramolecular charge-transfer molecules with great excited- and ground-state dipole-moment differences, Appl. Phys. Lett. 75 (1999) 28. doi:10.1063/1.124266.

[87] C.M. Isborn, A. Leclercq, F.D. Vila, L.R. Dalton, J.L. Brédas, B.E. Eichinger, B.H. Robinson, Comparison of static first hyperpolarizabilities calculated with various quantum mechanical methods, J. Phys. Chem. A. 111 (2007) 1319–1327. doi:10.1021/jp064096g.

[88] C.W. Dirk, M.G. Kuzyk, A Simplified Three-Level Model Describing the Molecular Third-Order Nonlinear Optical Susceptibility, Int. J. Quantum Chem. 43 (1992) 27–36. doi:CCC 0020-7608/92/0K0027.

[89] J.T. Gotro, S.A. Jenekhe, J.A. Osaheni, N. York, J.S. Meth, H. Vanherzeelef, Nonlinear Optical Properties of Poly (p -phenylenebenzobisoxazole), Chem. Mater. 4 (1992) 683–687. doi:0897-4756/92/2804-0683.

[90] C.W.D. M.G.Kuzyk, EfFects of centrosymmetry on the nonresonant electronic third-order nonlinear optical susceptibility, Phys. Rev. A. 41 (1990) 5098. doi:10.1103/PhysRevA.41.5098.

[91] S. Vidya, C. Ravikumar, I. Hubert Joe, P. Kumaradhas, B. Devipriya, K. Raju, Vibrational spectra and structural studies of nonlinear optical crystal ammonium D, L-tartrate: a density functional theoretical approach, J. Raman Spectrosc. 42 (2011) 676–684. doi:10.1002/jrs.2743.

[92] D.A. Kleinman, Nonlinear Dielectric Polarization in Optical Media, Phys Rev 1261977–1979. (1962) 1977–1979. doi:10.1103/PhysRev.126.1977.

[93] M.J. Paterson, O. Christiansen, F. Pawłowski, P. Jørgensen, C. Hättig, T. Helgaker, P. Sałek, Benchmarking two-photon absorption with CC3 quadratic response theory, and comparison with density-functional response theory, J. Chem. Phys. 124 (2006) 1–11. doi:10.1063/1.2163874.

[94] D.H. Friese, M.T.P. Beerepoot, M. Ringholm, K. Ruud, Open-ended recursive approach for the calculation of multiphoton absorption matrix elements, J. Chem. Theory Comput. 11 (2015) 1129–1144. doi:10.1021/ct501113y.

[95] M.T.P. Beerepoot, D.H. Friese, N.H. List, J. Kongsted, K. Ruud, Benchmarking two-photon absorption cross sections: performance of CC2 and CAM-B3LYP., Phys. Chem. Chem. Phys. 17 (2015) 19306–14. doi:10.1039/c5cp03241e.

[96] J.R. Hammond, K. Kowalski, Parallel computation of coupled-cluster hyperpolarizabilities, J. Chem. Phys. 130 (2009) 194108. doi:10.1063/1.3134744.

[97] K. Chaitanya, X.H. Ju, B.M. Heron, C.D. Gabbutt, Vibrational spectra and static vibrational contribution to first hyperpolarizability of naphthopyrans—A combined experimental and DFT study, Vib. Spectrosc. 69 (2013) 65–83. doi:http://dx.doi.org/10.1016/j.vibspec.2013.09.010.

[98] B. Skwara, R.W. Góra, R. Zaleśny, P. Lipkowski, W. Bartkowiak, H. Reis, M.G. Papadopoulos, J.M. Luis, B. Kirtman, Electronic Structure, Bonding, Spectra, and Linear and Nonlinear Electric Properties of Ti@C28, J. Phys. Chem. A. 115 (2011) 10370–

10381. doi:10.1021/jp206331n.

[99] R. Zaleśny, G. Wójcik, I. Mossakowska, W. Bartkowiak, A. Avramopoulos, M.G. Papadopoulos, Static electronic and vibrational first hyperpolarizability of meta-dinitrobenzene as studied by quantum chemical calculations, J. Mol. Struct. THEOCHEM. 907 (2009) 46–50. doi:http://dx.doi.org/10.1016/j.theochem.2009.04.011.

[100] M.G. Kuzyk, Fundamental limits of all nonlinear-optical phenomena that are representable by a second-order nonlinear susceptibility, J. Chem. Phys. 125 (2006) 1–11. doi:10.1063/1.2358973.

[101] J. Pérez-Moreno, Y. Zhao, K. Clays, M.G. Kuzyk, Modulated conjugation as a means for attaining a record high intrinsic hyperpolarizability., Opt. Lett. 32 (2007) 59–61. doi:10.1364/OL.32.000059.

[102] M.G. Kuzyk, Fundamental limits on third-order molecular susceptibilities, Opt. Lett. 25 (2000) 1183–1185. doi:10.1364/OL.25.001183.

[103] M.G. Kuzyk, Physical limits on electronic nonlinear molecular susceptibilities, Phys. Rev. Lett. 85 (2000) 1218–1221. doi:10.1103/PhysRevLett.85.1218.

List of Tables

Table 1 Observed absorption and computed vertical excitation for TPA BIZ and TPA BTZ.dyes in various solvents.

Dye	Solvent	Expt	TD-B3LYP/6-311+G(d,p)			
		λ_{max}	Vertical Excitation		Oscillator Strength (*f*)	Orbital Contribution
		nm	nm	eV		
TPA BIZ	Toluene	355	381	3.258	1.048	H→L (98%)
	Chlorofom	357	381	3.256	1.039	H→L (98%)
	EtOAc	350	380	3.263	1.020	H→L (98%)
	Acetone	352	380	3.259	1.019	H→L (98%)
	EtOH	350	380	3.259	1.020	H→L (98%)
TPA BTZ	Toluene	374	407	3.049	1.005	H→L (99%)
	Chlorofom	376	407	3.043	1.002	H→L (99%)
	EtOAc	370	407	3.050	0.987	H→L (99%)
	Acetone	375	407	3.045	0.994	H→L (99%)
	EtOH	371	407	3.045	0.995	H→L (99%)

Table 2 Observed emission and computed emission for TPA BIZ and TPA BTZ .dyes in various solvents

Dye	Solvent	Expt	TD-B3LYP/6-311+G(d,p)			
		λ_{max}	Emission		Oscillator Strength (*f*)	Orbital Contribution
		nm	nm	eV		
TPABIZ	Toluene	412	453	2.735	0.437	L→H (98%)

	Chlorofom	427	444	2.791	0.710	L→H (98%)
	EtOAc	414	443	2.802	0.725	L→H (98%)
	Acetone	427	442	2.807	0.802	L→H (98%)
	EtOH	432	442	2.807	0.808	L→H (98%)
	Toluene	434	506	2.450	0.274	L→H (99%)
TPABTZ	Chlorofom	458	495	2.506	0.445	L→H (99%)
	EtOAc	453	491	2.526	0.495	L→H (99%)
	Acetone	475	485	2.555	0.628	L→H (99%)
	EtOH	484	485	2.556	0.637	L→H (98%)

Table 3 Energy of HOMO, LUMO and band gaps of the TPABIZ and TPABTZ dyes in gas phase and solvents using TDDFT (B3LYP/6-311+G(d,p))method

Dye	Solvent	[a]LUMO (eV)	[b]HOMO (eV)	EL-EH(eV)	η
	Gas	-1.551	-5.344	3.79	1.90
	Toluene	-1.589	-5.363	3.77	1.89
	$CHCl_3$	-1.623	-5.386	3.76	1.88
TPA BIZ	EtOAc	-1.633	-5.393	3.76	1.88
	Acetone	-1.664	-5.416	3.75	1.88
	Ethanol	-1.666	-5.418	3.75	1.88
	Gas	-1.848	-5.407	3.56	1.78
	toluene	-1.903	-5.427	3.52	1.76
	$CHCl_3$	-1.945	-5.451	3.51	1.75
TPA BTZ	EtOAc	-1.956	-5.458	3.50	1.75
	Acetone	-1.991	-5.483	3.49	1.75
	Ethanol	-1.994	-5.485	3.49	1.75

[a] Energy of highest occupied molecular orbital (HOMO).

[b] Energy of lowest unoccupied molecular orbital (LUMO)

.

Table 4 Coupling strength (H_{DA}), coupling distance (R_{DA}), degree of delocalization C_b^2 and ratio of dipole moment for the TPA BIZ and TPA BTZ dyes in various solvents

Compound	TPA BIZ				TPA BTZ			
Solvent	$\mathbf{R_{DA}}$ **(Å)**	$\mathbf{H_{DA}}$ **(cm^{-1})**	C_b^2	μ_e/μ_g	$\mathbf{R_{DA}}$ **(Å)**	$\mathbf{H_{DA}}$ **(cm^{-1})**	C_b^2	μ_e/μ_g
Toluene	3.78	12425	1.06	0.80	4.00	11026	0.869	0.50
$CHCl_3$	3.75	12470	1.09	0.86	4.29	11414	0.974	0.47
EtOAc	3.71	12808	1.11	0.87	3.49	11406	0.927	0.50
Acetone	3.92	12447	1.02	0.90	4.37	11197	0.758	0.60
Ethanol	3.93	12389	1.02	0.91	3.81	10453	0.887	0.61

Table 5
Linear polarizability α_{CT} calculated by solvatochromic method and computed α_{CT} for TPA BIZ and TPA BTZ

	TPA BIZ				TPA BTZ			
		Computed α (× 10^{-24}) esu				Computed α (× 10^{-24}) esu		
Solvent	Expt	B3LYP	CAM B3LYP	BHHLYP	Expt	B3LYP	CAM B3LYP	BHHLYP
Toluene	17	32	31	30	19	30	29	29
$CHCl_3$	18	35	34	33	25	32	32	32
EtOAc	21	36	34	34	22	34	33	32
Acetone	15	39	37	36	21	37	35	35
Ethanol	18	39	37	37	16	37	36	35

Table 6
Total first order hyperpolarizability β_{CT} calculated by solvatochromic method and computed $method$ for TPA BIZ and TPA BTZ

	TPA BIZ				TPA BTZ			
		Computed β (× 10^{-30}) esu				Computed β (×10^{-30}) esu		
Solvent	Expt	B3LYP	CAM B3LYP	BHHLYP	Expt	B3LYP	CAM B3LYP	BHHLYP
Toluene	20	48	29	26	32	106	63	59
$CHCl_3$	22	62	37	33	41	133	77	73
EtOAc	24	66	39	35	35	141	81	76
Acetone	18	79	45	41	34	164	92	87
Ethanol	22	80	46	41	27	165	93	88

Table 7

Second order static hyperpolarizability obtained by solvatochromic and computational method

	TPA BIZ				TPA BTZ			
		Computed γ (× 10^{-36}) esu				Computed γ (× 10^{-36}) esu		
Solvent	Expt	B3LYP	CAM B3LYP	BHHLYP	Expt	B3LYP	CAM B3LYP	BHHLYP
Toluene	9	518	282	280	31	624	340	335
$CHCl_3$	8	658	349	346	31	813	430	422
EtOAc	6	697	368	364	27	865	455	446
Acetone	8	820	426	421	29	1032	533	522
Ethanol	10	831	431	426	28	1047	540	529

Table 8: Diagonal electronic and vibrational contributions to dipole polarizabilities and first hyperpolarizabilities of TPA BIZ and TPA BTZ obtained from of B3LYP/6-311+G(d,p) calculations in various solvent. (All values are in a.u.)

Dye	TPA BIZ					TPA BTZ				
Property	Toluene	$CHCl_3$	EtOAc	Acetone	Ethanol	Toluene	$CHCl_3$	EtOAc	Acetone	Ethanol
α_{xx}^{e}	640.4	681.5	691.8	721.7	724.1	686.1	733.8	745.8	780.8	783.6
α_{yy}^{e}	-3.3	-3.8	-3.9	-4.2	-4.2	-11.4	-12.8	-13.1	-14.2	-14.3
α_{zz}^{e}	393.4	428.4	437.8	467.0	469.4	404.1	442.1	452.4	484.2	486.8
α_{xx}^{v}	180.7	213.9	223.9	256.4	259.0	204.4	247.6	259.5	302.5	306.6
α_{yy}^{v}	94.9	108.5	113.0	128.3	129.6	82.3	96.4	100.2	112.6	113.8
α_{zz}^{v}	189.0	215.6	226.5	269.6	273.6	51.3	64.0	67.7	82.2	83.7
α^{e}	343.5	368.7	375.2	394.8	396.4	359.6	387.7	395.0	416.9	418.7
α^{v}	154.9	179.3	187.8	218.1	220.7	112.7	136.0	142.5	165.8	168.0
$\alpha^{e}+\alpha^{v}$	498.3	548.0	563.0	612.9	617.2	472.3	523.7	537.5	582.7	586.7
α^{v}/α^{e}	0.451	0.486	0.500	0.552	0.557	0.313	0.351	0.361	0.398	0.401
β_{xxx}^{e}	6974	8944	9482	11154	11293	-13829	17274	-18202	-21049	-21282
β_{yyy}^{e}	-53.4	-87.6	-98.7	-140.8	-144.8	-184.8	-227.5	-238.8	-272.5	-275.1
β_{zzz}^{e}	-1498	-1786	-1863	-2095	-2113	1489	1772	1847	2073	2092
β_{xzx}^{v}	-4072	-5164	-5427	-5933	-5944	4152	4805	4921	5016	4995
β_{yyy}^{v}	1565	-1697	1755	1931	1942	-1080	-1333	-1363	-1436	-1444
β_{zzz}^{v}	-4210	-4692	-4885	-5537	-5587	-2575	-3152	-3243	-3564	-3601
β^{e}	1808	2357	2507	2973	3012	-4175	6273	-5532	-6416	-6488

β^v	-2239	-3851	-2853	-3179	-3197	165.9	106.6	105.2	5.5	-16.8
$\beta^e+\beta^v$	-431.3	-1494.4	-345.6	-206.6	-184.9	-4009	6379	-5426	-6411	-6505
β^v/β^e	-1.239	-1.634	-1.138	-1.069	-1.061	-0.040	0.017	-0.019	-0.001	0.003

Table 9: Comparison of solvatochromic and theoretical values with the limiting values of hyperpolarizability for TPABIZ and TPABTZ

Solvent	β_{max} [a] ×(10^{-30} esu)	β_{CT} [b] × (10^{-30} esu)	β_0 [c] × (10^{-30} esu)	γ_{min} [d] × (10^{-36} esu)	γ_{max} [e] × (10^{-36} esu)	γ_{SD} [f] × (10^{-36} esu)	γ [g] × (10^{-36} esu)
TPABIZ							
Toluene	621	30	26	-518	2073	4	280
$CHCl_3$	568	31	33	-533	2132	1.4	346
EtOAc	454	30	35	-482	1931	1.9	364
Acetone	556	23	41	-672	2691	5.1	421
Ethanol	569	29	41	-690	2764	6.6	426
TPABTZ							
Toluene	745	48	59	-672	2691	33	335
$CHCl_3$	681	58	73	-690	2764	25	422
EtOAc	551	47	76	-637	2550	25	446
Acetone	561	46	87	-681	2727	30	522
Ethanol	543	36	88	-646	2585	33	529

a= limiting βmax values, b = solvatochromic β_{CT}, c = theoretical β0 from computation, d,e = limiting minimum and maximum γ values, f = solvatochromic γ, g = theoretical γ from computation.

List Of all Figures

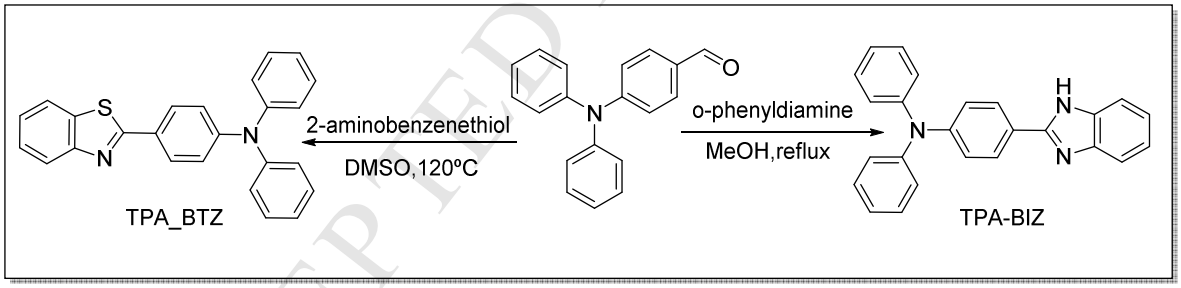

Fig 1. Synthesis of TPA BIZ and TPA BTZ

Fig 2 Absorption and Emission spectra of TPA BIZ and TPA BTZ

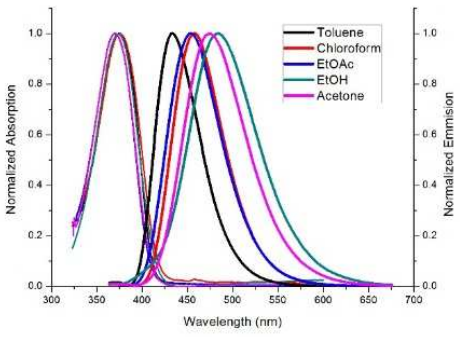

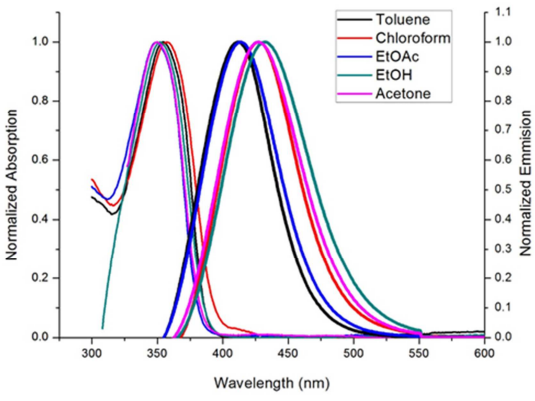

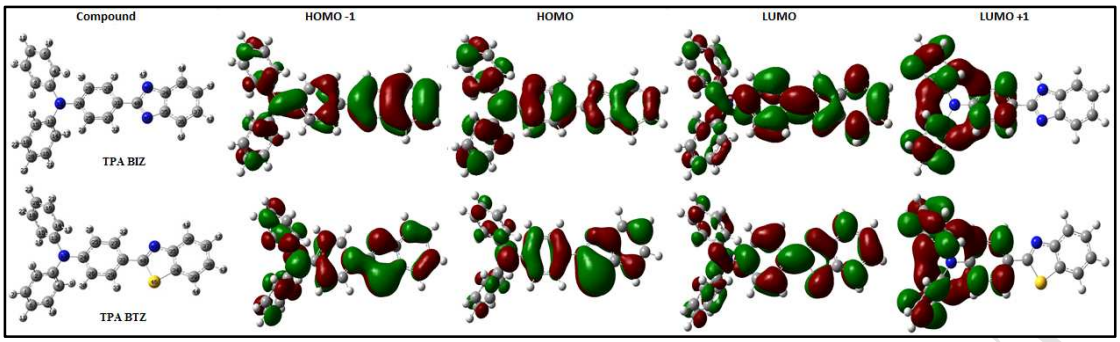

Fig 3 Frontier molecular orbitals of TPABIZ and TPABTZ dyes in the ground state

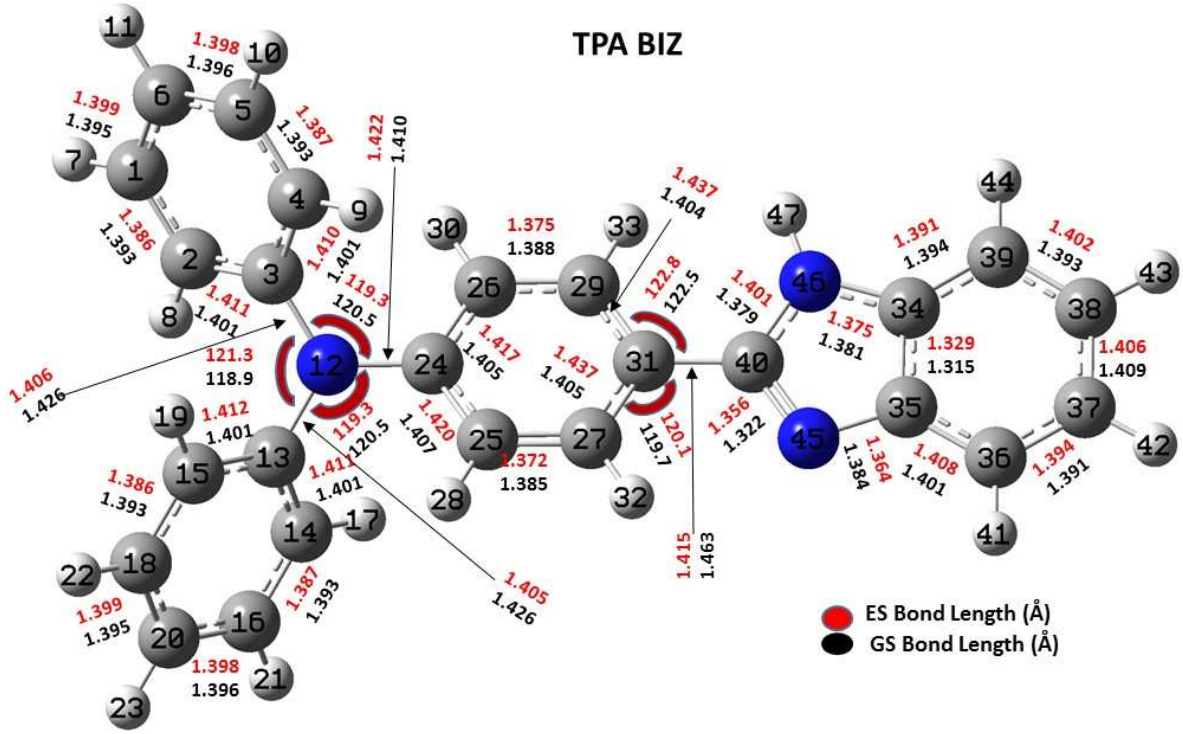

Fig. 4 Optimized geometry parameters of TPA BIZ dye in acetone solvent in the ground state and excited state (bond length are in Å, dihedral angles are in degree)

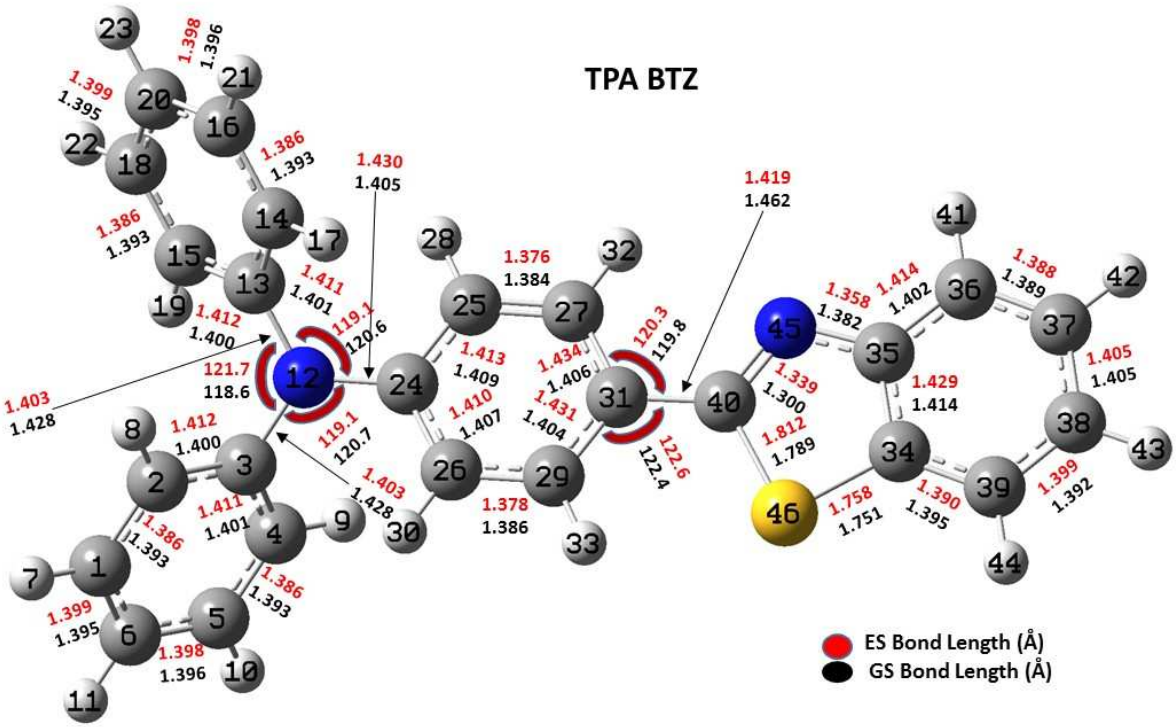

Fig. 5 Optimized geometry parameters of TPA BTZ dye in acetone solvent in the ground state and excited state (bond length are in Å, dihedral angles are in degree)

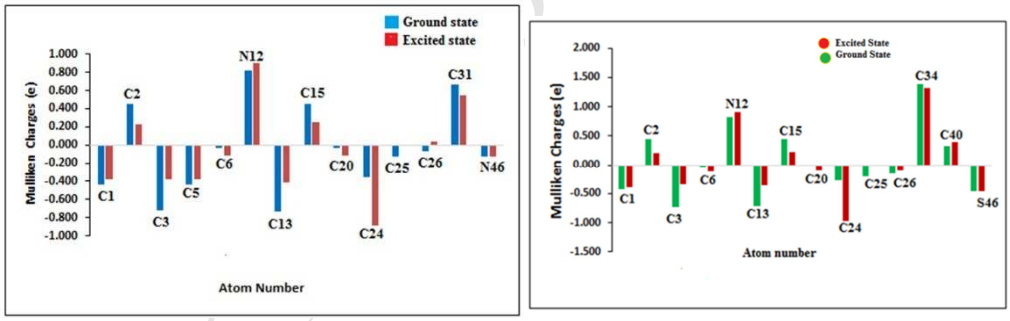

Fig 6 The ground state (GS) and excited state (ES) Mulliken charge (e) distribution of the compound TPA BIZ and TPA BTZ in Acetone

Highlights of Manuscript

1. DFT and Solvatochromic studies of triphenylamine based dyes
2. Calculations of first and second order hyperpolarizabilities.
3. NLO property evaluation of triphenylamine based dyes
4. Enhancement in NLO properties by introduction of Benzothiazole unit.